Comparative Infrared, *Raman*, and Natural-Bond-Orbital Analyses of *King*'s Sultam

by **Hans Hagemann**[a]), **Marcin Dulak**[a]), **Tomasz A. Wesolowski**[a]), **Christian Chapuis***[b])[1]), and **Janusz Jurczak**[b])[c])

[a]) Département de Chimie Physique, Université de Genève, 30 quai Ernest-Ansermet, CH-1211 Geneva 4
[b]) Institute of Organic Chemistry, Polish Academy of Sciences, Kasprzaka 44/52, PL-01-224
[c]) Department of Chemistry, University of Warsaw, Pasteura 1, PL-02-093

Dedicated to Dr. *Günther Ohloff* on the occasion of his 80th anniversary

By means of ^{1}H-NOESY- and *Raman*-spectroscopic analyses, we experimentally demonstrated the presence of the equatorial N–Me conformer of *King*'s sultam **4b** in solution, resulting from a rapid equilibrium. As a consequence, the value of the N lone-pair anomeric stabilization should be revised to 1.5–1.6 kcal/mol. Independently from the N tilting, natural bond orbital (NBO)-comparative analyses suggest that the S d* orbitals do not appear as primordial and stereospecific acceptors for the N lone pair. Second, the five-membered-ring sultams do not seem to be particularly well-stabilized by the S–C σ* orbital in the N-substituted *pseudo*-axial conformation, as opposed to an idealized *anti*-periplanar situation for the six-membered-ring analogues. In this latter case, the other *anti*-periplanar C–C σ* and C(1′)–H/C(2′) σ*orbitals are as important, if not more, when compared to the S–C σ* participation. In the *pseudo*-equatorial conformation, γ-sultams particularly benefit from the N lone-pair hyperconjugation with the *anti*-periplanar S–O_1 σ* and C(2)–H/C or C(1′)–H/C σ* orbitals. This is also the case for δ-sultams when the steric requirement of the N-substituent exceeds 1.6 kcal/mol. When both axial and equatorial conformations are sterically too exacting, the N-atom is prone to sp^2 hybridization or/and conformational changes (*i.e.*, **12c**). In that case also, the mode of stereoelectronic stabilization differs from γ- to δ-sultams.

Introduction. – Based on semi-empirical calculations, we proposed in [1] that the steric origin of the diastereoselectivity imparted to *N*-α,β-enoyl derivatives by γ-sultam auxiliaries of type **1**[2]) and **2** [6], as rationalized by *Kim* and *Curran* [7], is modulated by the stereoelectronic influence of the N lone pair (lp). We stressed that this additional effect, which is, under unchelating conditions, either matching or mismatching the steric approach, depending on the *syn*- or *anti*-s-*cis* conformations of the *N*-α,β-enoyl side chain, results from a general anomeric influence [8][3]) of the N lp, through the sp^2 C=O, on the LUMO π-facial electronic distribution of the reactive centers. The N lp is itself orientated by stabilization with the *anti*-periplanar S–O_1 σ* orbital. We later

[1]) Permanent address: Corporate R & D Division, *Firmenich* SA, P. O. Box 239, CH-1211 Genève 8.

[2]) For the original literature, see **1a** [2], **1b** [3], **1c** [4], **1d** [3], and **1e** [5].

[3]) For selected N lp through-bond and through-space directing interactions, initially suggested by *Müller* and *Eschenmoser*, see [9]. *Cieplak* proposed also an hyperconjugative influence of the N lp on the incipient bond-formation through the intermediacy of a sp^2-atom in Schemes 85, 86 as well as references 105 of [10]. For a hyperconjugative stabilization of ethane-staggered rotamers, see [11]. For validation of a hyperconjugative model by ^1J(C,H) NMR analysis [12] and influences on the bond lengths and electronegativity [13], evidenced by IR analysis, see [14]. For a negative hyperconjugative effect of the β-substituents on the α-deprotonation of sulfonyl derivatives, see [15].

synthesized and compared the X-ray structure [16] as well as the diastereoselectivities, imparted by the six-membered-ring sultam **3a**, during the *Diels-Alder* cycloaddition of its *N*,*N*′-bis fumaroyl derivative to cyclopentadiene [16], with those of its analogous congeners **1**, **2**, and **4**. On their side, *King et al.* [17] also invoked an anomeric effect, estimated between 2.0 and 2.5 kcal/mol. They based their rationalization on a stereoelectronic stabilization of the N lp with either the *anti*-periplanar, electronically deficient S–C σ^* [18] or the vacant S d orbitals [19], which favors bisection of the O=S=O angle by the N lp[4]). We now wish to report more details to compare these two opposite hypotheses, based on calculations at a higher *ab initio* level as well as conformational IR/*Raman* analyses of **4b**.

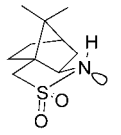

(–)-**1a**

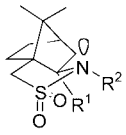

(–)-**1b** R^1=Me, R^2=H
(–)-**1c** R^1=H, R^2=F
(+)-**1d** R^1=Me, R^2=F
(–)-**1e** R^1=H, R^2=Me

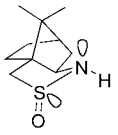

(–)-**2a**

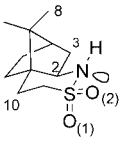

(–)-**3a**

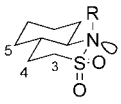

4a R=H
4b R=Me
4c R=F

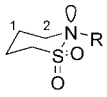

5a R=H
5b R=Me
5c R=F
5d R=Ph
5e R=4-$PhSO_2NH_2$

Results. – Based on X-ray structures as well as 300-MHz ^{1}H- and ^{13}C-NMR analyses at temperatures from 25° to −90°, *King et al.* attributed pure axial conformations to their δ-sultams **4a** and **4b** [17]. He argued that our hypothesis is biased by the steric influence of the Me(8) group at the N-atom, which precludes any conformation directing the N lp in a *pseudo*-equatorial direction[5]). We suggested rather that the axial orientations observed in their X-ray analyses could mainly result from either an intermolecular H-bond for **4a** (N–H ····· O=S)[6]) or external forces such as solid–solid packing interactions for **4b** [20]. We also refuted his argument by giving the example of the *N*-fluoro sultam **1c**, which exists in both *pseudo*-axial/equatorial conformations, as shown by ^{19}F-NMR analyses [4], thus leading us to suggest a more modest anomeric stabilization, estimated as $\leq$1.5 kcal/mol [16]. Furthermore, based on DFT calculations with *Becke–Perdew* functionals and DN** polarization basis set [21], we also suggested that their rigidified six-membered-ring sultam **4b** should, in solution, exist as

---

[4]) For an earlier example of *N*-benzyl axial δ-sultam, invoking this rationalization, see [20].
[5]) Private communications.
[6]) As also prudently underlined by Prof. *J. King* himself [17].

a mixture of axial and equatorial N–Me conformers. Finally, the calculated very low barrier of N-pyramidal inversion should account for the absence of observable distinct conformers on the NMR time scale (see *Table 1*). Although our ^{13}C-NMR and ^{1}H-NMR NOESY experiments on **4b** were fully consistent with *King*'s proposal, with respect to upfield γ-shifts of all three gauche C(3)-, C(4a)-, and C(8)-atoms as well as *Overhauser* interactions between the Me substituent and the axial H–C(8) (see *A*, in *Fig. 1*), H–C(4a) (*B*) and H–C(3) (*D*), we also later noticed interactions with the equatorial H–C(8) (*C*) and axial H–C(8a) (*E*), indicating a rapid equilibrium with the equatorial conformer. This hypothesis is further sustained by new *ab initio* calculations (see *Table 1*).

Further detailed and sophisticated ^{1}H- and ^{13}C-NMR analyses at 400, 500, and 600 MHz, by varying the temperature from 32° to −50°, confirmed our initial attributions[7]), but failed to uncover any new signals or dynamic processes[8]). These negative results, nevertheless, do not validate *King*'s hypothesis, since rapid N-pyramidal inversion necessitates alternative techniques such as ultrasonic relaxation measurement [22]. We, thus, turned our attention towards IR/*Raman* analysis and compared the experimental data collected for the pure crystalline axial conformer, either in solution or in the vapor phase, with both the vibrational frequencies of theoretical IR and *Raman* spectra of both axial and equatorial conformers derived from the B3LYP/6-31^{+}G** calculations.

The calculated harmonic frequencies and their assignment (where possible) for both axial and equatorial conformers are collected in *Table 4* (*Exper. Part*) together with the experimental frequencies measured in the gas phase (IR) and in the crystal (*Raman*). The corresponding spectra are shown in *Fig. 2* (IR) and *Fig. 4* (*Raman*) to facilitate comparisons. A $CDCl_3$ solution was preferred over $CHCl_3$ for the IR analysis, due to the absence of solvent absorption at *ca.* 3021 cm^{-1}.

For each N–Me axial and equatorial conformer considered, the calculated and experimental IR spectra of **4b** recorded in the gas phase (see *Fig. 3*, and *Table 4* in *Exper. Part*) are in good overall agreement. The patterns of the absorption bands are very similar. The positions of individual lines in the experimental and in the theoretical spectrum differ by less than 97 cm^{-1} for the lower band (below 1600 cm^{-1}). The entire theoretical high-frequency band (above 2900 cm^{-1}) is blue-shifted by *ca.* 120–170 cm^{-1} compared to the experimental spectrum. This band corresponds to various vibrational motions involving CH_2 and CH_3 groups. Harmonic frequencies of such vibrations calculated by DFT methods are known to be systematically overestimated by up to 4% for isolated organic molecules of medium size [23]. For this reason, it is the usual practice to scale the frequencies in order to facilitate comparisons with experiment. In our analyses, the frequencies are not scaled, because the scaling procedure is less justified in the low-frequency range, where the vibrational modes typically involve collective motions of several atoms of both rings.

---

[7]) For full attributions, see footnote 27 in [16].

[8]) We are particularly indebted to Prof. *U. Burger* and Dr. *D. Jeannerat* (University of Geneva) for these analyses beyond the limits of the NMR techniques. Indeed, a difference of less than 3.2 kcal/mol, for the N-pyramidal inversion, corresponds approximately to the rotational barrier of ethane, which is unobservable by this spectroscopic method.

Table 1. Ab initio *Energy Differences* [kcal/mol] *between Axial, Planar, and Equatorial Minimized Conformers of* King*'s Sultam* **4b**

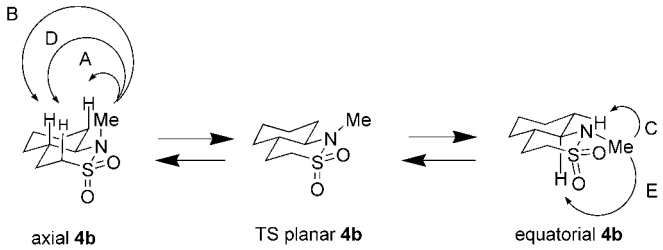

axial **4b** TS planar **4b** equatorial **4b**

BP/DN** [16]	+0.08	+1.7	0.00
PWP91/6-31G**	+0.59	+3.2	0.00
B3LYP/6-31G**	+0.70	+2.9	0.00
B3LYP/6-31^{+}G**	+0.71	+3.1	0.00
B3LYP/lacv3p**$^{++}$	+0.62	+2.7	0.00

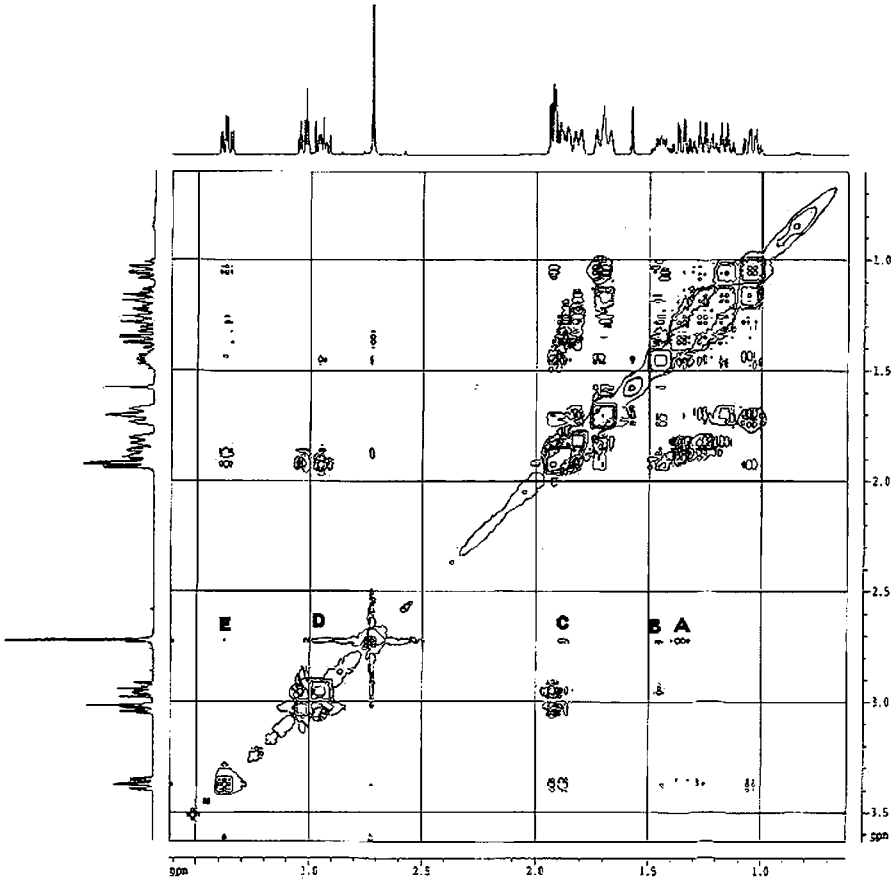

Fig. 1. *^{1}H-NMR NOESY Experiment on* **4b** *in $CDCl_3$ solution*

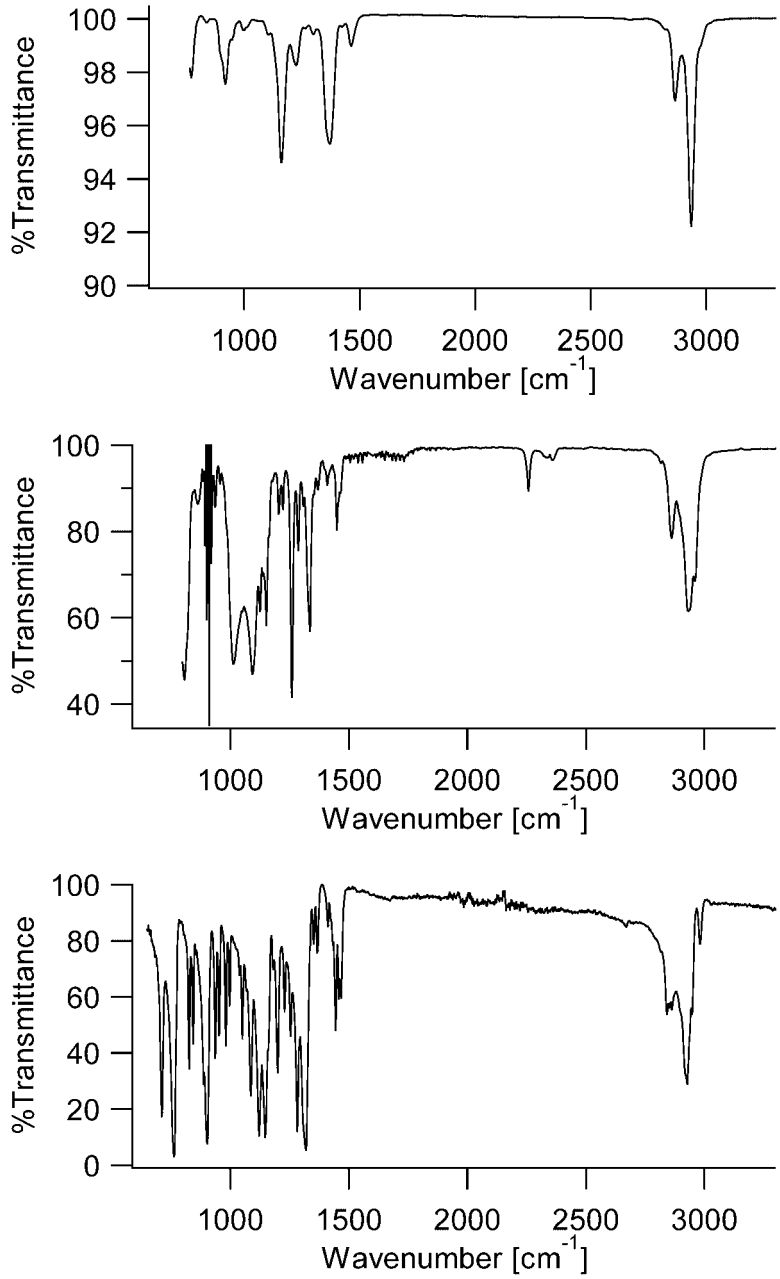

Fig. 2. *IR Survey spectra of* **4b** *in the gas phase at* ca. *250°* (top), *in 3% $CDCl_3$ solution* (center), *and as crystal* (bottom)

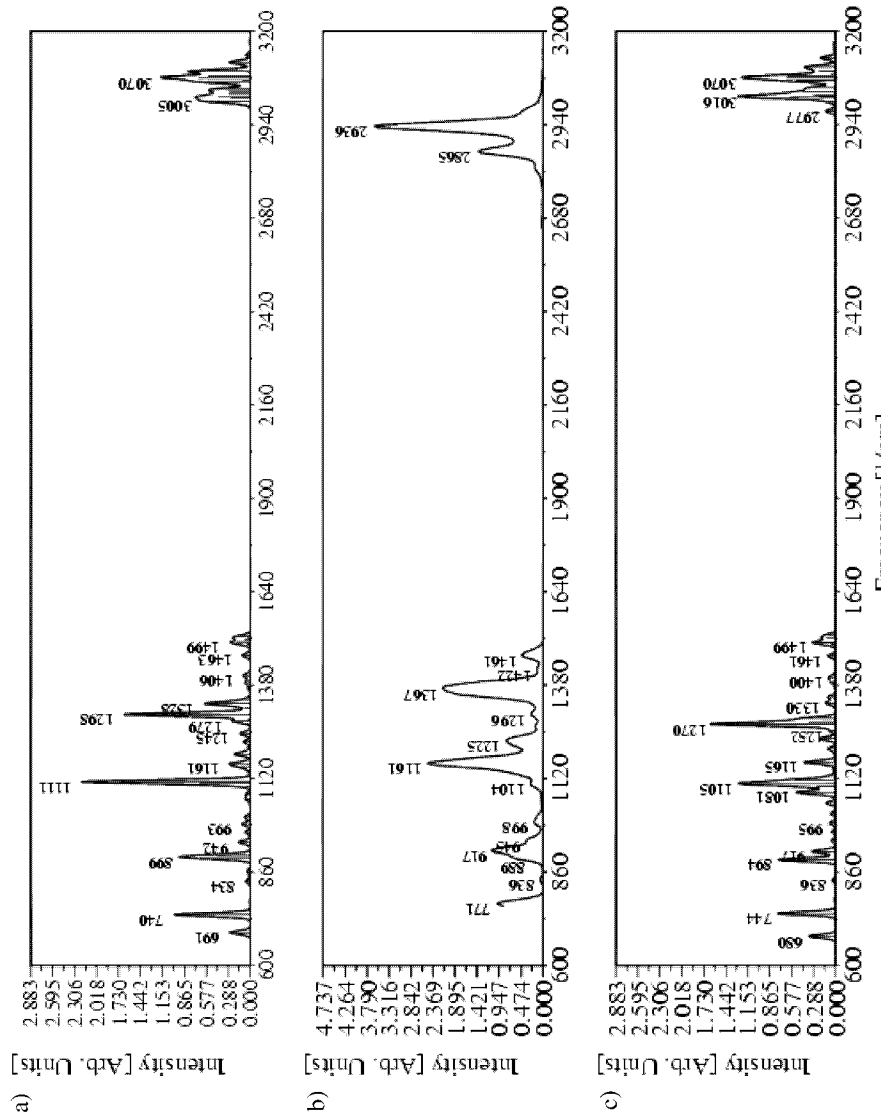

Fig. 3. *IR Frequencies and intensities of the axial conformer* **4b** (*a*, calculated), *of* **4b** *in the vapor phase* (*b*, experimental), *and of the equatorial conformer* **4b** (*c*, calculated)

Second, since the shift differences between the data collected in the crystalline state and those obtained from the solution are very small, the presence of the equatorial conformer could statistically not be confirmed on the basis of *ipso*- and bathochromic shifts[9]). A certain number of frequencies are noteworthy to discuss since their variations exceed the resolution of our equipment, estimated to be at the best *ca.* 3 cm^{-1}. Interestingly, the 1320(cryst.)/1336(soln.)/1364(gas) bands principally find their origin in the asymmetric SO_2 stretching[10]), while the symmetric SO_2 stretching is relatively stable at 1148(cryst.)/1151(soln.)/1153(gas) cm^{-1}. Depending on the conditions, the CH_2 absorptions are more shifted at 1088(cryst.)/1095(soln.)/1104(gas) than at 1052(cryst.)/1049(soln.)/1055(gas) cm^{-1}. We also compared the respective intensities of the observed IR bands with the calculated values. The theoretical spectra for both conformers considered are very similar. It is, therefore, rather difficult to use them to identify a predominant conformer. Nevertheless, we detected in the IR spectrum a unique feature, which differentiates the theoretical spectra of both conformers. It is the overall shape of the high-frequency band. The two most pronounced experimental bands in this region (*Table 4* in *Exper. Part*) correspond to the modes involving the CH_2 and CH_3 groups: the experimental strong band at *ca.* 2936 cm^{-1} is attributed to carbocyclic CH_2 stretching, whereas the experimental medium band at *ca.* 2865 cm^{-1} is due to CH_2 stretching and asymmetric stretching of CH_3. This pattern is similar for all three conditions (cryst./soln./gas) and suggests, in contrast to calculations (*Table 1*), the predominance of the axial conformer.

We, thus, decided to proceed to a dynamic study by varying the temperature and, therefore, turned towards a laser *Raman* study, which is often complementary to IR analysis. Indeed, since the vibration frequencies are obtained indirectly by irradiating the sample with monochromatic visible light, and since the intensity of a *Raman* line is given by the rate of change of the molecular polarizability as the atoms pass through equilibrium, *Raman* spectra can often supply missing data.

With respect to *Raman* spectra, the experimental spectrum is available only for the low-frequency range. As for the IR, a good overall agreement between the theoretical spectra of either conformers and the experimental data can be seen (*cf. Fig. 5*). The deviations between the position of theoretical and experimental frequencies do not exceed 32 cm^{-1}. The uniform shift of *ca.* 3 cm^{-1} between both *Raman* experiments at 25° suggests an experimental reference displacement in the same order of magnitude as the resolution of our apparatus and, unfortunately, does not allow us to discuss shift modifications. As the N–Me bending at 336(cryst.)/337(soln.) cm^{-1} falls right at the foot of the solvent absorption, we focused our attention at a pair of skeletal vibrations involving the SO_2 moiety at 495(cryst.)/501(soln.) and 528(cryst.)/531(soln.) cm^{-1}, since their calculated values suggest a change in their respective intensities (indicated

---

[9]) Indeed, only ten on twenty ipsochromic and two on six bathochromic shifts (underlined and *italics* values in the *Exper. Part*, resp.) are observed as compared to the calculated displacements resulting from the hypothetical presence of the equatorial conformer **4b** in solution.

[10]) Although the frequencies are determined primarily by the forces within the molecule, they are also affected by intermolecular forces. Minor differences are, therefore, to be expected between the spectra of the same substance in the gaseous, liquid, and solid states. The shift of the asymmetric SO_2 stretching of *ca.* 10 to 20 cm^{-1} on going from the solid to solution has already been reported [24]. Differentiated IR analyses of optically pure *vs.* racemic substrates forming conglomerates are also well-known [25].

by an asterisk in *Fig. 4*). Indeed, the pure crystalline, axial conformer exhibits a medium signal at 495 cm^{-1} and a stronger one at 528 cm^{-1}. Decreasing the temperature from 50° (*D* in *Fig. 4*) to 25° (*C*) and −30° (*B*) resulted in a modification of both respective signal intensities, consistent with the decrease in population of the equatorial conformer of **4b** in solution. Indeed, this latter is expected to be responsible for a smaller intensity of the 501-cm^{-1} band with respect to that at 531-cm^{-1}. Computer analysis of all three curves confirmed the visual intensity change but, due to the strong fluorescence, resulting in a relatively moderate signal-to-noise ratio, allied to the fact that both bands are not representative of pure conformers but composed of superimposed signals [26], did not allow us to precisely calculate the difference in conformational energy. We can only conclude that this difference is very small, in agreement with tendencies found in the results of various *ab initio* and DFT-type calculations (see *Table 1*)[11]). Furthermore, this tiny difference of N−Me axial/equatorial conformational energies found for **4b** may well be below the standard error of *ab initio* calculations for unusual sulfonamide functionalities, thus rendering perilous any assignment of the major conformer based on these energy differences derived from theoretical calculations. The pattern of the intensities of these two bands either at low

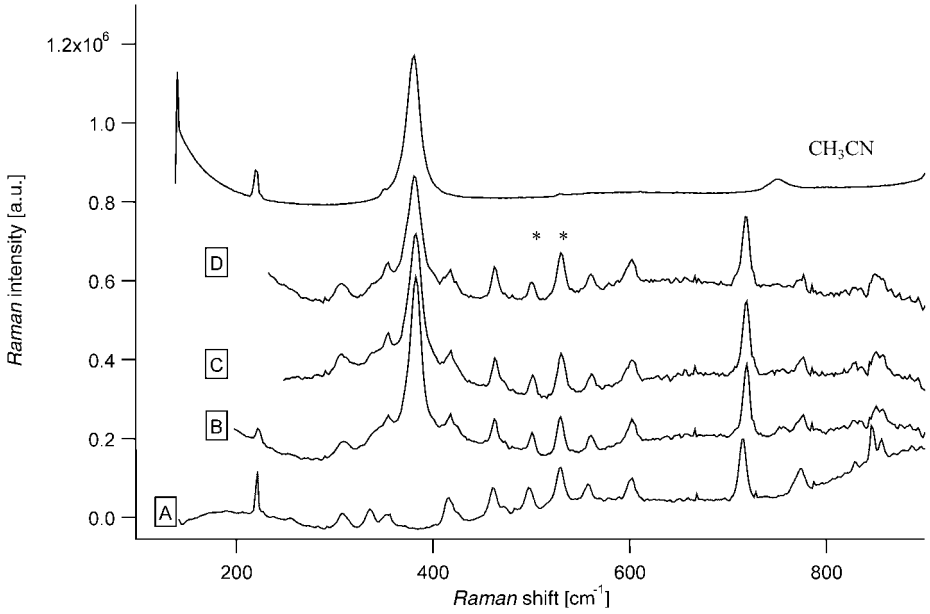

Fig. 4. *Raman analysis of crystalline* **4b** *at 25°* (A), *of a 10% MeCN solution of* **4b** *at −30°* (B), *25°* (C), *and 50°* (D), *with solvent absorption*

[11]) Besides uncertainties in assessing the integrated absorption coefficient of the conformer bands, determination of the thermodynamic parameters of a system involving variable-temperature IR or *Raman* measurements is complicated by the possible 'natural decrease' of the band intensities with increasing temperature [27]. Furthermore, a polar solvent such as $CDCl_3$/$CHCl_3$ or MeCN may modify the stereoelectronic stabilization/polar interactions and, consequently, the conformational ratio [28].

temperature or in the crystalline state resembles more the calculated spectrum for the axial conformer. The other feature distinguishing the two conformers is the pattern of intensities in the low-frequency *Raman* spectrum. The intensity pattern for the two conformers differs significantly in the 300–370-cm^{-1} range. The 336-cm^{-1} band is attributed to the CH_2 vibrations in the carbocycle for both conformers, and to CH_3 and SO_2 vibrations for the axial conformer only. The 353-cm^{-1} band is attributed to CH_2, CH_3, and SO_2 vibrations for the axial conformer, and to CH_3 and SO_2 for the equatorial conformer. The 368-cm^{-1} band is attributed to CH_2 and SO_2 vibrations for both conformers, and to CH_3 for the axial conformer (see *Table 4* in *Exper. Part*). The pattern of intensities for the axial conformer (*Fig. 5,a*) closely resembles the experimental one (*Fig. 5,b*) recorded from crystalline sultam **4b**. Since these three vibrational modes involve atoms differing in geometry in the axial and equatorial conformers, we consider the detected difference in the intensity pattern to be a strong indication for the predominance of the axial conformer, as shown by X-ray analysis [17].

Discussion. – Having experimentally established the presence of the equatorial conformer **4b** in solution[12]), hence the pertinence of our calculations, suggesting both a small difference of conformational and interconversional energies, we then turned our attention to the second part of our hypothesis, namely the origin of the N lp stabilization.

The NBO analyses (*Table 2*) were performed on the comparative examples that we initially discussed [16]. These *ab initio* calculations confirmed a more stable *pseudo*-equatorial conformation for the crystalline, free sultams **1a** and **1b** [16], in which the stereoelectronic stabilization mainly originates in both *anti*-periplanar S–O(1), and C(2)–H or C(2)–Me σ^* orbitals. For their minor *pseudo*-axial conformers, their N lp is partially stabilized by the *anti*-periplanar C(2)–C(1), and, to a smaller extent, by the S–C and S–O(1) σ^* orbitals. The stabilization brought by the S d* orbitals is moderate and practically of a similar order of magnitude, independent of the conformation adopted by **1a** and **1b**. Although reduced by the electronegativity of the halogen, the *N*-fluoro analogues **1c** and **1d** show the same stereoelectronic features. Noteworthy are the conformational energies of both thermodynamically more stable pseudo-equatorial *N*-fluoro sultams, in line with the values expected from their respective ^{19}F-NMR [4][3] or X-ray[13]) analyses. Due to the absence of a *pseudo*-equatorial S=O functionality, the case of sulfinamide **2a** is peculiar. Indeed, the strong S–O(1) and C(2)–H σ^* contributions are determinant in both conformations, the S–C influence being modest in comparison with either the C(2)–C(1) σ^* or even the S d* orbitals. The latter is a more efficient acceptor for the N lp in the *pseudo*-equatorial conformers of the γ-sultams **1a**–**1d** and sulfinamide **2a**. Finally, the case of the *N*-Me sultam **1e** follows the same trends, although we were unable to compare it with its pseudo-axial conformer, due to expected severe steric interactions with the Me(8) substituent. The case of the

---

[12]) For conformational studies, involving enthalpic differences of 0.5–0.7 kcal/mol, based on *Raman* analyses of well-separated signals, see [29]; for measurements of rotamer populations, estimated by IR spectroscopy, see [30].

[13]) See footnote 22 in [16].

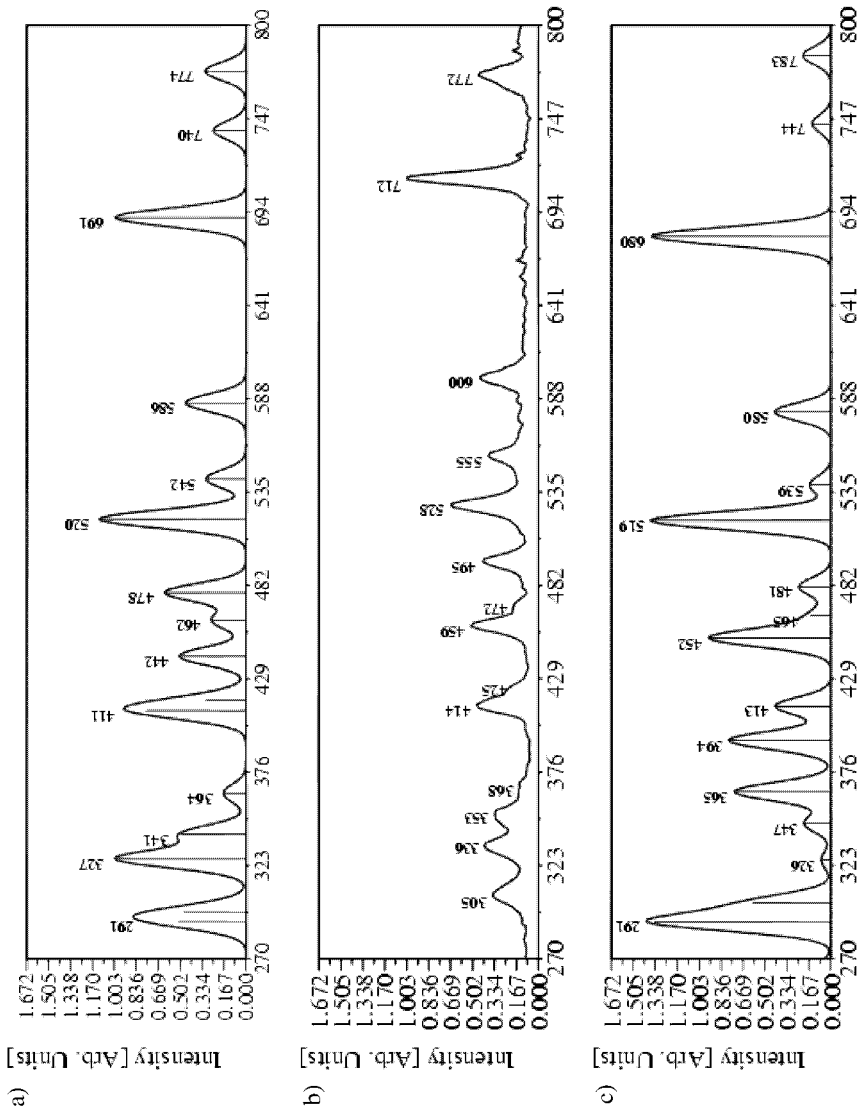

Fig. 5. *Raman Frequencies and intensities of the axial conformer* **4b** (*a*, calc.), *of crystalline* **4b** (*b*, exper.), *and of the equatorial conformer* **4b** (*c*, calc.)

Table 2. *NBO Analyses for N lp as Donor with the Common Most Efficient Acceptors, after B3LYP/6-31G**/lacv3p**++ Minimization*

	Pseudo-axial or axial												
[kcal/mol]	**1a**	**1b**	**1c**	**1d**	**2a**	**3a**	**4a**[a])	**4b**[a])	**4c**[a])	**5a**[b])	**5b**[b])	**5c**[b])	**1e**
Conform. ΔE	0.87	1.56	1.49	4.68	3.03	1.28	0.24	1.09		0.36	1.83		$\gg 5$
S 3d*[c])	2.84	2.86	1.30	1.19	2.81	3.69	3.71	3.79	2.23	3.69	3.90	2.32	
C(2) 2p*[d])	0.78	0.72	1.79	1.74	0.87				0.88	1.57	1.62	1.99	
C(2) 3d*[c])	0.89	1.64			1.65	0.54	1.44	**4.92**	0.78				
H–N 1s*	1.27	1.28			1.21	1.12	1.33			1.18			
S–C σ*	3.55	3.34	1.80	1.54	1.21	**6.29**	**6.16**	**6.57**	2.93	**6.09**	**6.60**	2.88	
S–O(1) σ*	3.47	3.75	0.70	1.78	**5.67**	2.57	2.50	2.75		2.48	3.03		
S–O(2) σ*								0.55	0.90			0.84	
C(2)–C(3) σ*					0.85			0.59	0.54				
C(2)–C(1) σ*	**4.98**	**4.75**	**4.87**	3.84	3.70	**7.28**	**6.74**	**6.95**	**5.08**	**6.69**	**6.88**	**5.14**	
C(2)–H_{ax} σ*	3.24		1.28		**4.98**	2.91	1.78	1.70		1.95[e])	2.13[e])	1.17[e])	
C(2)–Me_{ax} σ*		2.06		0.84									
C(1′)–H σ*[f])								**7.37**			**7.61**		
	Pseudo-equatorial or equatorial												
[kcal/mol]	**1a**	**1b**	**1c**	**1d**	**2a**	**3a**	**4a**[a])	**4b**[a])	**4c**[a])	**5a**[b])	**5b**[b])	**5c**[b])	**1e**
Conform. ΔE									1.83			1.65	
S 3d*[c])	2.93	3.17	1.50	1.63	3.16	2.24	2.22	2.11	1.58	2.15	2.71	1.54	3.08
C(2) 2p*[d])	1.17	0.93	1.50	1.65	1.28	1.15	0.99	0.90	1.34	1.06	2.18		0.80
C(2) 3d*[c])		0.74	0.62		0.64	0.59							0.51
H–N 1s*	1.44	1.19			1.13	1.20	1.06			1.07			
S–C σ*					1.26	1.12	1.25		1.22	1.19			
S–O(1) σ*	**6.65**	**5.76**	2.84	2.71	**7.51**	**8.45**	**8.39**	**8.10**	**4.29**	**8.39**	**8.18**	**4.22**	**7.07**
S–O(2) σ*	2.36	3.70	1.37	2.04		0.70	0.79	0.73	0.89	0.73	0.83	0.86	2.31
C(2)–C(3) σ*	1.19	1.89	0.58	0.87	0.87								
C(2)–C(1) σ*						0.88	1.46	1.53		1.39	1.38		1.04
C(2)–H_{ax} σ*	**6.23**		3.65		**6.21**	**6.05**	**6.38**	**6.18**	**4.43**	**5.98**	**6.15**	3.91	**7.08**
C(2)–Me_{ax} σ*		**6.52**		**5.13**									
C(1′)–H σ*[f])								**6.23**			**6.25**		**6.03**

[a]) C(1) = C(4a), C(2) = C(8a), C(10) = C(3). [b]) Arbitrarily numbered in order to correspond with (−)-**3a**. [c]) $d_{xy} + d_{yz} + d_{x^2y^2} + d_{z^2}$. [d]) $p_x + p_y + p_z$. [e]) Equatorial C(2)–H. [f]) C(1′) = *Me*–N.

crystalline six-membered-ring, free sultam **3a** is also noteworthy. Indeed, although the equatorial N–H conformer exhibits an excellent stabilization of its N lp by the axial S–O(1) and C(2)–H σ* orbitals in comparison with the efficient S–C and C(2)–C(1) σ* orbitals of its axial conformer, we clearly see, in this latter case, a nonnegligible contribution of the S d* orbitals. This feature is confirmed by the NBO analysis of the *trans*-decalenic sultams **4a** and **4b**. In addition, the axial conformer of the *N*-Me δ-sultam **4b** is worthy of discussion. Indeed, apart from the increased S d* and S–O(2) σ* contributions, this conformer also profits from both substantial additional C(2) d* as well as C(Me)–H σ* stabilizations. This latter interaction results from a much better *anti*-periplanar, staggered disposition as compared to the equatorial conformer, sterically hindered by, amongst others, the SO_2 moiety. We also took into account the *N*-fluoro analogue **4c**, since the conformation of this unreported compound should not

be influenced by intermolecular H-bonds[14]). Calculations indicate that the axial conformer should be the most stable, thus moderating our interest in its possible synthesis and X-ray analysis, as it would not be a determinant proof in favor of *King*'s hypothesis. In contrast to previous rationalizations, it should be underlined that, in all these series, the factors for S d* and S–C σ* contributions are smaller than the *anti*-periplanar C(2)–C(1) σ* stabilization. The same conclusions are reached from the NBO analyses of the known oily, six-membered-ring sultams **5a** and **5b** [31][32], and unreported *N*-fluoro sultam **5c**. In accord with *ab initio* calculations, both ^{1}H- and ^{13}C-NMR analyses (δ 2.91 and 23.95 ppm, resp.) of δ-sultam **5b** suggest, in solution, the participation of an equatorial conformation for the *N*-Me substituent [33][15]).

To extend both the foundations and scope of our conclusions, we completed this NBO study by a search in the *CCDC* database (2002). In addition to both equatorial, sterically demanding *N*-aryl δ-sultams **5d** and **5e** [35][36], already discussed by *King et al.* to estimate their value of anomeric stabilization, we exhumed two supplementary instructive and comparative examples of five- and six-membered-ring sultams[16]).

The first couple is represented by the *cis*-fused five- and six-membered-ring bicyclic sultams **6** and **7** [46], which both possess a conformationally anchoring *pseudo*-equatorial, more stable Ph substituent on the cyclohexene part. Interestingly, despite the absence of the geminal dimethyl moiety of the bornyl skeleton[17]), the γ-sultam **6** orients its *N*-benzyl substituent in a *pseudo*-equatorial, thermodynamically slightly more stable conformation (0.28 kcal/mol; *Table 3*). In contrast, its δ-homologue **7** exhibits a by 1.30 kcal/mol less-stable, axial conformer in the crystalline state. We should here keep in mind the limit of reliance (*vide supra*) attributable to such low theoretical difference of conformational energies! For both sultams and conformations, the NBO analyses show medium but undiscriminating influence of the S d* orbitals as N lp acceptor. In addition to the C(1′)–H σ*, the *pseudo*-equatorial conformer of **6** is mainly stabilized by the *pseudo*-axial S–O(1) and C(2)–H σ* orbitals. Interestingly, its *pseudo*-axial conformer is not stabilized by the S–C σ* orbital but rather by the *pseudo*-equatorial S–O(2) and C(2)–H σ* orbitals, the influence of the C(1′)–H σ* stabilization being slightly less pronounced. Although less efficiently hyperconjugated, the six-membered-ring, equatorial sultam **7** shows similar features, while the axial conformer is distinctly favored by the *anti*-periplanar S–C and C(2)–C(1) σ* orbitals

---

[14]) For intermolecular H-bonds directing the N tilting in the X-ray analyses of (–)-**1a**, (–)-**2a**, (–)-**3a**, see [16].

[15]) Furthermore, in contrast to rigidified **4b**, the entropic term for the additional interconversion of the six-membered ring of monocyclic **5b** should also be considered. For the five-membered-ring analogues of **5a** and **5b**, see [34].

[16]) For X-ray structures of γ-sultams possessing a *pseudo*-equatorial *N*-ethyl or *N*-cyclohexyl substituent, see [37] and [38], resp. For structurally restricted sultams possessing a bridgehead N lp bissecting the O=S=O angle, see [39]. For *N*-aryl (2*R*)-bornane-10,2-sultams, see [40]. For non-N–C=O substitutions of this auxiliary, see [41]. For a bicyclo[2.2.2]octene homologue of **8**, resulting from an *endo*-IMDA cycloaddition, see [42]. For five- and six-membered-ring benzosultams, see [43]. For potential intramolecular H-bonding of a five-membered-ring, free sultam, see [44]. For structure determination and intermolecular H-bond analyses of a sulfonamide, based on powder diffraction data associated with solid-state NMR, see [45].

[17]) See *Footnote 5* for *King*'s steric argument. Structures, conformations, and diastereoselectivities imparted by *N*-unsubstituted and *N*-substituted γ-sultams derived from (3a*R*)-7,7-dimethyl-4,5,6,7-tetrahydro-3*H*-3a,6-methano-2,1-benzisothiazole-2,2-dioxide [47] shall be reported in due course with the corrective X-ray-analysis of **1a**.

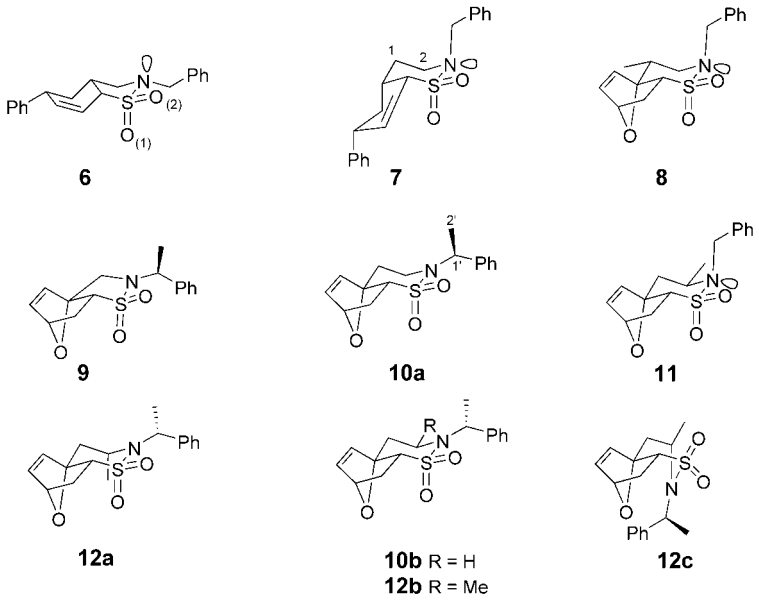

Table 3. *NBO Analyses for Lp(N) as Donor with the Common Most Efficient Acceptors, after B3LYP/6-31G**/lacv3p**++ Minimization*

	Pseudo-equatorial or equatorial					*Pseudo*-axial or axial					Planar N	
[kcal/mol]	**5d**	**6**	**7**	**8**	**11**	**5d**	**6**	**7**	**8**	**11**	**9**	**10a**
Conform. ΔE					0.58	1.64	0.28	1.30	1.46			
S 3d*[a])	2.99	3.36	2.81	2.92	2.70	3.30	3.31	3.56	3.63	3.70	2.35	**4.59**
C(2) 2p*[b])	1.23	1.21	1.07	1.42	0.79	0.95	1.03	0.81	0.90	0.95	0.70	1.41
C(1′) 2p*[b])		1.08	1.47	1.53	1.11	1.21[c])	0.98	0.51	0.53	0.92	1.40	0.61
C(2′) 2p*[b])											**4.19**	
S–C σ*	1.50	0.52	1.26	1.32	1.35	**5.93**	**6.46**	**6.60**	**6.72**		**6.59**	
S–O(1) σ*	**7.71**	**8.88**	**8.38**	**8.82**	**8.31**	**4.41**	3.08	3.87	**4.03**	**4.15**	**5.11**	**5.52**
S–O(2) σ*	0.62	2.11	0.81	0.87	0.68		**7.34**				**6.80**	
C(2)–C(1) σ*	1.87		1.66	2.23	1.97	**6.37**	0.65	**6.45**	**6.89**	**6.96**		**7.22**
C(2)–H_{ax} σ*	**5.97**	**6.48**	**5.73**	**5.43**	**4.87**	3.26	1.48	0.71	1.84	1.55	**7.93**	2.72
C(2)–H_{eq} σ*			2.74					**6.81**	2.34	1.11	0.85[d])	2.91
0.86												
C(1′)–H σ*		**6.93**	**5.93**	**5.88**	**5.23**		**6.67**	**7.03**	**7.35**	**5.15**	1.50	
C(1′)–C(2′) σ*	**8.42**[e])					**6.69**[e])					**7.43**	**6.44**
C(1′)–C_{arom} σ*	**5.12**[f])	1.60	1.83	1.70	2.45	**13.52**[f])	1.51	2.34	2.00	3.92	1.11	3.64

[a]) $d_{xy} + d_{yz} + d_{x^2y^2} + d_{z^2}$. [b]) $p_x + p_y + p_z$. [c]) C(1′) = C_{ipso} arbitrarily numbered in order to correspond with (–)-**3a**. [d]) Equatorial C(2)–Me. [e]) C_{ipso}–C_{ortho} + C_{ipso}–C'_{ortho} σ*. [f]) C_{ipso}–C_{ortho} π*.

in addition to a much more efficient geometrically well oriented C(1′)–H *anti*-bonding σ* orbital. Similar conclusions may be extracted from both structurally related axial *N*-benzyl crystalline sultams **8** and **11** [20]. It is noteworthy that the axial conformer of **11**, in contrast to **8**, is thermodynamically more stable by 0.58 kcal/mol with respect to its

equatorial conformer, due to the additional steric influence of the equatorial Me substituent at C(2). The second example deals with the sterically more-demanding and planar *N*-α-methylbenzyl sultams **9** and **10a** [48]. When we tried to calculate both their axial and equatorial N sp^3 conformers, the resulting N hybridization was invariably automatically readjusted to sp^2 [18]). Their NBO analyses show remarkable differences with respect to the benzyl analogues **6** and **7**.

The planar γ-sultam **9** differs notably from its six-membered-ring analogue **10a** by an efficient stabilization of the N lp by the C(2′) 2p*, S−O(2) σ*, C(2)−H_{ax}, and C(1′)−C(2′) σ* orbitals. The δ-sultam **10a** is characterized by efficient S−C and C(2)−C(1) σ* acceptors, while the C(1′)−C(2′) σ* and S d* orbital influences are not negligible.

Conclusions. – By ^{1}H-NOESY and *Raman*-spectroscopic analyses, we experimentally demonstrated the presence, in solution, of the equatorial *N*-Me conformer of *King*'s sultam **4b**, thus confirming our *ab initio* calculations of a rapid thermodynamic equilibrium. The intensities of the signals observed in these analyses (*B vs. E* in *Fig. 1*, at 2865 *vs.* 2936 cm^{-1} in *Fig. 3*, and at 501 *vs.* 531 cm^{-1} in *Fig. 4*) are consistent with the predominance of the axial conformer **4b** in solution, in contrast to theoretical calculations performed at $-273°$, suggesting a slightly more-stable ($\leq$1.1 kcal/mol; *Tables 1* and *2*) equatorial conformer with a low barrier of N-pyramidal interconversion ($\leq$ 3.2 kcal/mol). This dichotomy may result from at least three reasons: *a*) a minor environment effect resulting from the interactions with either solvent molecules in the liquid phase ($CDCl_3$ for NMR and IR, or MeCN for *Raman* analyses) or neighboring molecules in the crystal as compared to the gas phase equilibrium; *b*) the effect of the solvent on the intensity, completely neglected in our calculations; *c*) inaccuracy of our approximations, such as exchange-correlation functional, harmonic approximation for frequencies, double harmonic approximation for intensities, or incomplete basis sets. As a consequence of this equilibrium, the value of the N lp anomeric stabilization earlier estimated between 2.0–2.5 kcal/mol [17] should be, as we suggested [16], revised to 1.5–1.6 kcal/mol. This value is close to that usually measured for anomeric stabilization of acetals or aminals [8]. With respect to the origin of this anomeric stabilization, we should distinguish between five- and six-membered-ring sultams. Indeed, independently from the N tilting, NBO comparative analyses indicate that the S d* orbitals do not appear as primordial and specific stereo-acceptors for the N lp. Second, based on the examples considered, the five-membered-ring sultams do not seem to be particularly well-stabilized by the S−C σ* orbital in the *pseudo N*-substituted axial conformation, as opposed to an idealized *anti*-periplanar situation of the N lp for the six-membered-ring analogues. In this latter case, the other *anti*-periplanar C−C σ* or C(1′)−H/C(2′) orbitals are as important, if not more, when compared to the S−C σ* participation. In the *pseudo*-equatorial conformation, γ-

---

[18]) The other diastereoisomers **12a** and **12b** also exhibit a planar sp^2 N. This steric effect even imposes a boat conformation on diastereoisomer **12c** [48]. For sp^3 *N*-α-methylbenzyl *pseudo*-equatorial five-membered-ring sultams, see [49]. Calculations for the unreported *N*-isopropyl analogues of **9** and **10a** suggest a sp^3 N *pseudo*-equatorial conformation favored by 6.44 and 4.87 kcal/mol over their constrained *pseudo*-axial conformers, respectively.

sultams particularly well benefit from the N lp *anti*-periplanar S–O(1) σ^* and C(2)–H/C or C(1′)–H/C σ^* delocalization. As a result, this more effective stabilization positively influences a *pseudo*-equatorial conformation, even in the absence of the sterically demanding geminal dimethyl moiety of the bornane skeleton (*i.e.*, see **6** *vs.* **7**). In the case of the *N*-alkyl six-membered-ring sultams, one of the decisive contributions, besides the slightly higher acceptance of the S d* orbitals, may be attributed to a very efficient *anti*-periplanar C(1′)–H/C σ^* hyperconjugation, resulting from the staggered geometry of their N-axial conformers. This *anti*-periplanarity is altered in the equatorial conformation by the steric influence of the SO_2 moiety. In absence of such a potential stereoelectronic stabilization, like in the case of the sterically deviated *N*-^{i}Pr analogue of **10a**, or when the steric influence of the *N*-substituent exceeds 1.6 kcal/mol, the conformation of δ-sultams tends to adopt an equatorial conformation either in solution or in the crystalline state, with stereoelectronic stabilization by the S–O(1) and C–H/C *anti*-periplanar σ^* orbitals[19]). When both axial/equatorial conformations are sterically too exacting, the N-atom is prone to sp^2 hybridization. In that case also, the mode of stereoelectronic stabilization differs from γ- to δ-sultams. The latter undergo an increased influence of their S d* orbitals, while the former show a poor S–C σ^* stabilization. These NBO calculations support our initial hypothesis with respect to the five-membered-ring sultams, while *King*'s hypothesis may be applied to six-membered-ring analogues.

Having rationalized the hyperconjugative effect of the N lp on the conformations of the γ- and δ-sultams **1**–**12**, we shall now concentrate on demonstrating its stereoelectronic influence on the reactive centers of their *N*-alkenoyl derivatives. Although we have argued for this supplementary rationalization for several years [1], this concept has not been yet well accepted and recognized[20]). This results from the fact that most of the diastereoselective reactions studied involve the C=O α-atom [52], which is directly under the steric influence of the chiral auxiliary [7]. We recently demonstrated that this influence is extremely tenuous on the more-distant reactive β-center, even in the case of a restricted conformation [53] or of a cumulative co-operative effect [54]. As a consequence, we shall now explore diastereoselective 1,4-additions to *N*-cinnamoyl derivatives of **1a**, suitably modified in the *para*-position by an electronically influential substituent. The resulting diastereoselectivities *vs. Hammett* parameters shall be reported in due course.

We are particularly indebted to Dr. *S. March* (University of Geneva) for IR measurements and Prof. *J. King* for his pertinent comments on the manuscript and for bringing our attention to the inverted S–N and S–C distances reported for **1a** [16][17]). The access to the computational resources at the *Swiss Center for Scientific Computations* in Manno is greatly acknowledged.

---

[19]) Despite an excellent C_{ipso}–C_{ortho} π^* stabilization of the N lp in the *pseudo*-axial conformation of Ph δ-sultam **5d**, this latter adopts an equatorial conformation due to the steric demand of the Ph substituent (1.64 kcal/mol in the axial conformation; see *Table 3*). It is noteworthy that *King et al.* overestimated this steric effect by comparison with an α-unsubstituted Ph-cyclohexane (2.5–3.0 kcal/mol). For a discussion of the *gauche*-interactions of the SO_2 moiety with the equatorial *N*-substituent in δ-sultams, see [16]. For electronic *vs.* steric influences on the conformational equilibria of cyclohexyl esters, see [50].

[20]) For exceptions, see, *e.g.*, [51].

Table 4. *Theoretical Frequencies* [cm^{-1}] (B3LYP/6-31$^+$G**) *of Axial and Equatorial Conformers and Experimental Bands of* King*'s Sultam* **4b** *in Solid* (*Raman*, 25°) *and Vapor Phase* (IR, *ca.* 250°)

Axial	Description (Axial)	*Raman*	IR	Description (Equatorial)	Equatorial
3113	CH_3 asym. str.			CH_3 asym. str.	3125
				CH_2 in ring 2[a])	3100
				CH_2 in ring 1	3090
3088	CH_2				
3074; 3070, 3059[b])	CH_2 in ring 2		2936*s*	CH_2 in ring 2	3075, 3070, 3062[b])
3033, 3025, 3017, 3013[b])	CH_2 in ring 2		2865*m*	CH_2 in ring 2	3030, 3022, 3019[b])
3005	CH_3 asym. str.			CH_3 asym. str.	3016
				C−H str.	2977
1514	CH_2 in ring 2, CH_3 rock		1461*m*	CH_2 in ring 2, CH_3 rock	1518
1507	CH_2, CH_3 rock			CH_3 rock	1512
1499	CH_2, CH_3		1450*m*	CH_2, CH_3	1499
1463	CH_2 bend., CH_3 umbrella		1422*w*	CH_2 bend.	1461
1298	CH_2, SO_2 asym. str.		1367*s*	CH_2	1287
1279	CH_2			CH_2, SO_2 asym. str.	1270
1245			1296*w*		1252
1222					1230
1188			1260*w*		1202
1161			1225*m*		1165
1111	CH_2, SO_2 sym. str., CH_3		1161*s*	CH_2, CH_3, C−N	1115
1107	CH_2, SO_2 sym. str.			CH_2, SO_2 sym. str., CH_3	1105
1098	CH_2, C−C		1104*w*	CH_2	1081
1063	CH_2		1055*w*	CH_2, C−C	1051
993	CH_2, CH_3, C−C		998*w*	CH_2, CH_3, C−C	995
942	CH_2, C−C		945*w*	CH_2, CH_3	917
899	CH_2, CH_3		917*m*	CH_2, CH_3	899
			889*w*		
834	CH_2		836*w*	CH_2	836
740	CH_2, CH_3, C−S−N asym. str.	772*m*	771*m*	CH_2, CH_3, C−S−N asym. str.	744
691	CH_2, CH_3, C−S	712*s*		CH_2, CH_3, C−S−N sym. str.	680
586		600*m*			580
542	SO_2 bend., CH_2	555*m*		SO_2 bend., CH_2	539
520		528*s*			519
478		495*m*			481
462		472*w*			465
442		459*m*			452
417		425*w*			413
411		414*m*			394
364	CH_2, SO_2, CH_3	368*w*		CH_2, SO_2,	365
341	CH_2, CH_3, SO_2	353*m*		CH_3, SO_2	347
327	CH_2 in ring 2, CH_3, SO_2	336*m*		CH_2 in ring 2	326
297	CH_2, CH_3, SO_2	305*m*		CH_2, CH_3, SO_2	302
291	CH_2, CH_3, C−S−N bend.			CH_2, CH_3, C−S−N bend.	291
180	CH_3 rock			CH_3 rock	243

[a]) Ring 1 contains the N-atom. [b]) Several close-lying wavelengths are grouped together because all of them can be attributed to the vibrations of the same groups.

Experimental Part

General. See [55]. For NBO analyses [56], the 4.0-version of the JAGUARD software (Ed. 2000; *Schrödinger Inc.*, Portland, OR, USA) was used on a PC-compatible *Pentium* bi-processors computer. Orbitals (B3LYP/lacv3p**$^{++}$) were calculated after minimization of the geometry (B3LYP/6-31G**). *Raman* spectra were obtained with a *Holospec* spectrometer equipped with a liq. N_2-cooled CCD camera. The Ar ion laser (488 nm, power less than 100 mW) was focussed with a cylindrical lens on a glass capillary containing the sample. The unpolarized spectra were obtained in a backscattering geometry. For the measurements at 25 and 50°, the capillary was placed in a brass holder, which was thermostated with a circulating water bath. For measurements below r.t., the sealed capillary tube with the soln. was fixed to the cold finger of a *Dewar* cooled with a dry ice/acetone mixture. All spectra presented a very strong luminescence background, which was subtracted using a polynomial interpolation.

The harmonic fundamental frequencies, IR intensities, and *Raman* scattering activities of the axial and equatorial conformers have been obtained from density-functional-theory (DFT) calculations using B3LYP [57] exchange-correlation functional and 6-31$^+$G** basis set (*Table 4*). The basis set was chosen taking into account the fact that accurate calculations of *Raman* intensities by DFT methods are known to require large basis sets comprising polarized and diffused functions [58]. Gaussian 98 suite of programs was used [59]. Geometry was optimized using a tight convergence criterion for the first derivative (0.000050 *Hartree/Bohr* or *Hartree/Radian*). The absolute differential *Raman* scattering cross-sections were calculated from the *Raman* scattering activities, as described in [60]. To facilitate comparisons between the calculated spectra (represented as pairs of frequencies and the corresponding intensities) and the experimental ones, the theoretical ones were convolved with the Gaussian-type functions with a full-width half-maximum (FWHM) equal to 12 cm^{-1} (for IR and *Raman*). The spectra were normalized with respect to the heights of the well-separated experimental lines at 771 (for IR) and 712 cm^{-1} (for *Raman*) and the corresponding theoretical lines in the case of calculated spectra.

IR Analysis [cm^{-1}] *of Crystalline* **4b** *at 25°*[9]): 2982*w*, 2935*m*, 2928*s*, *2863m*, 2842*m*, 1467*m*, 1458*m*, 1446*m*, *1413w*, 1369*w*, 1352*w*, 1320*s*, 1308*w*, 1284*s*, 1256*m*, *1230w*, 1202*s*, 1182*w*, 1148*s*, 1123*s*, 1088*s*, *1052m*, 1040*w*, 998*w*, *982m*, 955*m*, 938*m*, 904*s*, 889*m*, 845*m*, *828m*, 765*s*, 713*s*.

IR Analysis [cm^{-1}] *of* **4b** *in 1% $CHCl_3$ Soln. at 25°, 0.25-mm Cell:* 3021*m*, 2938*s*, 2928*m*, 2862*m*, 1468*w*, 1458*m*, 1449*m*, 1411*w*, 1373*w*, 1358*w*, 1337*s*, 1305*w*, 1288*m*, 1255*w*, 1224*m*, 1203*w*, 1192*w*, 1151*s*, 1126*s*, 1091*m*, 999*w*, 989*w*, 958*w*, 938*m*, 909*s*, 888*m*, 846*w*, 825*m*, 765*m*, 714*s*, 666*m*.

IR Analysis [cm^{-1}] *of* **4b** *in 3% $CDCl_3$ Soln. at 25°, 0.25-mm Cell*[9]): 2960*s*, 2931*s*, *2862m*, 1468*w*, 1460*w*, 1450*m*, *1410w*, 1371*w*, 1358*w*, 1336*s*, 1309*w*, 1288*m*, 1261*s*, *1223m*, 1206*m*, 1185*w*, 1153*s*, 1127*s*, 1095*s*, *1049m*, 1015*s*, *980w*, 958*w*, 939*w*, 906*s*, 889*w*, 865*w*, *808s*.

Raman *Analysis* [cm^{-1}] *of* **4b** *in 10% MeCN Soln. at 25°*: 775*m*, 719*s*, 603*m*, 561*w*, 531*s*, 501*m*, 463*m*, 418*m*, 354*w*, 337*w*, 306*w*.

REFERENCES

[1] a) C. Chapuis, J.-Y. de Saint Laumer, presented at the 'IX ESOC', Warsaw, Poland, June 1995; b) T. Bauer, C. Chapuis, J. Kiegiel, J. W. Krajewski, K. Piechota, Z. Urbanczyk-Lipowska, J. Jurczak, *Helv. Chim. Acta* **1996**, *79*, 1059; c) T. Bauer, C. Chapuis, A. Jezewski, J. Kozak, J. Jurczak, *Tetrahedron: Asymmetry* **1996**, *7*, 1391; d) C. Chapuis, J.-Y. de Saint Laumer, M. Marty, *Helv. Chim. Acta* **1997**, *80*, 146; e) C. Chapuis, A. Kucharska, J. Jurczak, *Tetrahedron: Asymmetry* **2000**, *11*, 4581; f) S. Szymanski, C. Chapuis, J. Jurczak, *Tetrahedron: Asymmetry* **2001**, *12*, 1939.

[2] W. Oppolzer, C. Chapuis, G. Bernardinelli, *Helv. Chim. Acta* **1984**, *67*, 1397.

[3] E. Differding, R. W. Lang, *Tetrahedron Lett.* **1988**, *29*, 6087; E. Differding, W. Frick, R. W. Lang, P. Martin, C. Schmit, S. Veenstra, H. Greuter, *Bull. Soc. Chim. Belg.* **1990**, *99*, 647.

[4] F. A. Davis, P. Zhou, C. K. Murphy, G. Sundarababu, H. Qi, W. Han, R. M. Przelawski, B. C. Chen, P. J. Carroll, *J. Org. Chem.* **1998**, *63*, 2273.

[5] R. L. Shriner, J. A. Shotton, H. Sutherland, *J. Am. Chem. Soc.* **1938**, *60*, 2794.

[6] C. Chapuis, R. Kawecki, Z. Urbanczyk-Lipkowska, *Helv. Chim. Acta* **2001**, *84*, 579.

[7] B. H. Kim, D. P. Curran, *Tetrahedron* **1993**, *49*, 293.

[8] a) R. U. Lemieux, *Pure Appl. Chem.* **1971**, *25*, 527; b) E. L. Eliel, *Angew. Chem., Int. Ed.* **1972**, *11*, 739; c) J.-M. Lehn, G. Wipff, *Helv. Chim. Acta* **1978**, *61*, 1274; d) A. J. Kirby, 'The Anomeric Effect and Related Stereoelectronic Effects at Oxygen', in 'Reactivity and Structure Concepts in Organic Chemistry', Springer

Verlag, Berlin, 1983, Vol. 15, p. 71; e) S. Li, A. J. Kirby, P. Deslongchamps, *Tetrahedron Lett*. **1993**, *34*, 7757; f) S. Li, P. Deslongchamps, *Tetrahedron Lett*. **1993**, *34*, 7759; g) J. F. King, R. Rathore, Z. Guo, M. Li, N. C. Payne, *J. Am. Chem. Soc*. **2000**, *122*, 10308.

[9] K. Müller, A. Eschenmoser, *Helv. Chim. Acta* **1969**, *52*, 1823; A. Vasella, *Helv. Chim. Acta* **1977**, *60*, 1273; A. Kümin, E. Maverick, P. Seiler, N. Vanier, N. Damm, R. Hobi, J. D. Dunitz, A. Eschenmoser, *Helv. Chim. Acta* **1980**, *63*, 1158; A. G. Schulz, J. J. Napier, *Tetrahedron Lett*. **1982**, *23*, 4225; P. Magnus, T. Gallagher, P. Brown, J. C. Huffman, *J. Am. Chem. Soc*. **1984**, *106*, 2105; A. I. Meyers, B. A. Lefker, K. T. Wanner, R. A. Aitken, *J. Org. Chem*. **1986**, *51*, 1936; A. I. Meyers, M. A. Seefeld, B. A. Lefker, J. F. Blake, *J. Am. Chem. Soc*. **1997**, *119*, 4565.

[10] A. S. Cieplak, *Chem. Rev*. **1999**, *99*, 1265.

[11] V. Pophristic, L. Goodman, *Nature* **2001**, *411*, 565; V. Pophristic, L. Goodman, *J. Phys. Chem*. **2002**, *106*, 1642.

[12] G. Cuevas, E. Juaristi, *J. Am. Chem. Soc*. **2002**, *124*, 13088.

[13] I. V. Alabugin, T. Zeidan, *J. Am. Chem. Soc*. **2002**, *124*, 3175.

[14] L. Enxiang, P. Xin, L. Ruwei, T. Yurong, J. Zhongsheng, W. Gecheng, L. Yongsheng, H. Ninghai, *Guangpuxue Yu Guangpu Fenxi* **2000**, *20*, 31 (*Chem. Abstr.* **2000**, *132*, 293461).

[15] J. F. King, M. C. Li, Z. Allan, V. Dave, N. C. Payne, *Can. J. Chem*. **2003**, *81*, 638.

[16] A. Piatek, C. Chapuis, J. Jurczak, *Helv. Chim. Acta* **2002**, *85*, 1973; A. Piatek, C. Chapuis, J. Jurczak, *J. Phys. Org. Chem*. **2003**, *16*, 700.

[17] J. F. King, G. Yuyitung, M. S. Gill, J. C. Stewart, N. C. Payne, *Can. J. Chem*. **1998**, *76*, 164; J. F. King, K. C. Khemani, S. Skonieczny, N. C. Payne, *J. Chem. Soc., Chem. Commun*. **1988**, 415.

[18] W. v. E. Doering, L. K. Levy, *J. Am. Chem. Soc*. **1955**, *77*, 509; D. W. J. Cruickshank, *J. Chem. Soc*. **1961**, 5486; R. M. Moriarty, *Tetrahedron Lett*. **1964**, 509; R. M. Moriarty, *J. Org. Chem*. **1965**, *30*, 600; W. N. Speckamp, U. K. Pandit, P. K. Korver, P. J. van der Haak, H. O. Huisman, *Tetrahedron* **1966**, *22*, 2413; H. P. Klug, *Acta Crystallogr., Sect. B* **1968**, *24*, 792; W. B. Jennings, R. Spratt, *J. Chem. Soc., Chem. Commun*. **1970**, 1418; T. S. Cameron, K. Prout, B. Denton, R. Spagna, E. White, *J. Chem. Soc., Perkin Trans. 2* **1975**, 176; J. F. King, 'The Chemistry of Sulfonic Acids, Esters and their Derivatives', Eds. S. Patai, Z. Rappoport, John Wiley & Sons, 1991, p. 249.

[19] S. Wolfe, A. Stolow, L. A. Lajohn. *Tetrahedron Lett*. **1983**, *24*, 4071; D. A. Bors, A. Streitwieser, *J. Am. Chem. Soc*. **1986**, *108*, 1397; T. Laube, T. A. Ha, *J. Am. Chem. Soc*. **1988**, *110*, 5511; M. Moklesur-Rahman, D. M. Lemal, *J. Am. Chem. Soc*. **1988**, *110*, 1964; J. Elguero, P. Goya, I. Rozas, J. Catalean, J. L. De Paz, *J. Mol. Struct*. (*Theochem*) **1989**, *184*, 115; P. Groner, J. R. Durig, in 'Cyclic Organonitrogen Stereodynamics', Eds. J. B. Lambert, Y. Takeuchi, VCH, New York, 1992, p. 31; R. Koch, E. Anders, *J. Org. Chem*. **1994**, *59*, 4529; M. B. Blanca, E. Maimon, D. Kost, *Angew. Chem., Int. Ed*. **1997**, *36*, 2216.

[20] P. Metz, D. Seng, R. Frohlich, B. Wibbeling, *Synlett* **1996**, 741.

[21] A. D. Becke, *Phys. Rev*. **1988**, *38*, 3098; J. P. Perdew, *Phys. Rev*. **1986**, *33*, 8822.

[22] E. Wyn-Jones, R. A. Pethrick, *Top. Stereochem*. **1970**, *5*, 269; A. R. Katritzky, R. C. Patel, F. G. Riddell, *Angew. Chem., Int. Ed*. **1981**, *20*, 521; A. M. Belostotskii, H. E. Gottlieb, M. Shokhen, *J. Org. Chem*. **2002**, *67*, 9257.

[23] G. Rauhut, P. Pulay, *J. Phys. Chem*. **1995**, *99*, 3093.

[24] J. N. Baxter J. Cymerman, J. B. Willis, *J. Chem. Soc*. **1955**, 669.

[25] J. Jacques, A. Colet, S. H. Wilen, in 'Enantiomers, Racemates and Resolutions' Krieger Publ. 1991, Malabar, Florida, p. 18, 80.

[26] D. J. Chadwick, J. Chambers, R. L. Snowden, *J. Chem. Soc., Perkin Trans. 2* **1974**, 1181.

[27] D. J. Chadwick, J. Chambers, R. Macrae, G. D. Meakins, R. L. Snowden, *J. Chem. Soc., Perkin Trans. 2* **1976**, 597.

[28] M. Chmielewski, J. N. BeMiller, D. P. Cerretti, *J. Org. Chem*. **1981**, *46*, 3903.

[29] H. Hagemann, J. Mareda, C. Chiancone, H. Bill, *J. Mol. Struct*. **1997**, *410*, 357.

[30] G. A. Guirgis, B. R. Drew, N. J. Luangjamekorn, S. Shen, J. R. Durig, *J. Mol. Struct*. **2002**, *613*, 15; W. A. Herrebout, C. Zheng, B. J. van der Veken, J. R. Durig, *J. Mol. Struct*. **2003**, *645*, 109.

[31] H. Feichtinger, *Chem. Ber*. **1963**, *96*, 3068; J. T. Doi, W. K. Musker, *J. Org. Chem*. **1985**, *50*, 1.

[32] E. M. Kaiser, P. L. A. Knutson, *J. Org. Chem*. **1975**, *40*, 1342.

[33] E. I. Troyanskii, M. I. Lazareva, V. E. Zubarev, A. I. Lutsenko, G. I. Nikishin, *Bull Acad. Sci. USSR Div. Chem. Sci*. **1988**, *37*, 1401.

[34] A. D. Bliss, W. K. Cline, C. E. Hamilton, O. J. Sweeting, *J. Org. Chem*. **1963**, *28*, 3537; J. F. King, S. M. Loosmore, M. Aslam, J. D. Lock, M. J. Mc Garrity, *J. Am. Chem. Soc*. **1982**, *104*, 7108; E. H. White, H. M. Lim, *J. Org. Chem*. **1987**, *52*, 2162; J. Lee, Y.-L. Zhong, R. A. Reamer, D. Askin, *Org. Lett*. **2003**, *5*, 4175.

[35] B. Helferich, K. G. Kleb, *Liebigs Ann. Chem.* **1960**, *635*, 91; B. Helferich, V. Boellert, *Liebigs Ann. Chem.* **1961**, *647*, 37; A. McIntosh, B.Sc. Thesis, University of Western Ontario, 1990.
[36] J. Aupers, C. H. Carlisle, P. F. Lindley, *Acta Crystallogr., Sect. B* **1974**, *30*, 1228; A. Camerman, C. Camerman, *Can. J. Chem.* **1975**, *53*, 2194.
[37] M. Inagaki, T. Tsuri, H. Jyoyama, T. Ono, K. Yamada, M. Kobayashi, Y. Hori, A. Arimura, K. Yasui, K. Ohno, S. Kakudo, K. Koizumi, R. Suzuki, M. Kato, S. Kawai, S. Matsumoto, *J. Med. Chem.* **2000**, *43*, 2040.
[38] T. Iwama, M. Ogawa, T. Kataoka, O. Muraoka, G. Tanabe, *Tetrahedron* **1998**, *54*, 8941.
[39] H. J. Breternitz, E. Schaumann, G. Adiwidjaja, *Tetrahedron Lett.* **1991**, *32*, 1299; L. A. Paquette, S. M. Leit, *J. Am. Chem. Soc.* **1999**, *121*, 8126; M. J. Uddin, M. Kikuchi, K. Takedatsu, K. Arai, T. Fujimoto, J. Motoyoshiya, A. Kakehi, R. Iriye, H. Shirai, I. Yamamoto, *Synthesis* **2000**, 365; L. A. Paquette, Choon Sup Ra, J. D. Schloss, S. M. Leit, J. C. Gallucci, *J. Org. Chem.* **2001**, *66*, 3564.
[40] C. Kandzia, E. Steckhan, F. Knoch, *Tetrahedron: Asymmetry* **1993**, *4*, 39; Z. Gross, S. Ini, *Inorg. Chem.* **1999**, *38*, 1446; M. Moreno-Manas, R. M. Sebastian, A. Vallribera, J. F. Piniella, A. Alvarez-Larena, M. L. Jimeno, J. Elguero, *New J. Chem.* **2001**, *25*, 329.
[41] W. Oppolzer, G. Poli, C. Starkemann, G. Bernardinelli, *Tetrahedron Lett.* **1988**, *29*, 3559; W. Oppolzer, C. Starkemann, I. Rodriguez, G. Bernardinelli, *Tetrahedron Lett.* **1991**, *32*, 61; J. H. Rigby, P. Sugathapala, M. J. Heeg, *J. Am. Chem. Soc*. **1995**, *117*, 8851; V. Srirajan, V. G. Puranik, A. R. A. S. Deshmukh, B. M. Bhawal, *Tetrahedron* **1996**, *52*, 5579.
[42] B. Plietker, D. Seng, R. Frohlich, P. Metz, *Tetrahedron* **2000**, *56*, 873.
[43] K. H. Ahn, H. H. Baek, S. J. Lee, C. W. Cho, *J. Org. Chem*. **2000**, *65*, 7690; Y. Misu, H. Togo, *Org. Biomol. Chem*. **2003**, *1*, 1342.
[44] J. Wanner, A. M. Harned, D. A. Probst, K. W. C. Poon, T. A. Klein, K. A. Snelgrove, P. R. Hanson, *Tetrahedron Lett.* **2002**, *43*, 917.
[45] M. Rajeswaran, T. N. Blanton, N. Zumbulyadis, D. J. Giessen, C. Conesa-Moratilla, S. T. Misture, P. W. Stephens, A. Huq, *J. Am. Chem. Soc.* **2002**, *124*, 14450.
[46] I. R. Greig, M. J. Tozer, P. T. Wright, *Org. Lett.* **2001**, *3*, 369.
[47] W. Treibs, I. Lorenz, *Chem. Ber*. **1949**, *82*, 400; U. Verfürth, I. Ugi, *Chem. Ber*. **1991**, *124*, 1627.
[48] V. O. Rogatchov, H. Bernsmann, P. Schwab, R. Fröhlich, B. Wibbeling, P. Metz, *Tetrahedron Lett.* **2002**, *43*, 4753.
[49] K. F. Ho, D. C. W. Fung, W. Y. Wong, W. H. Chan, A. W. M. Lee, *Tetrahedron Lett*. **2001**, *42*, 3121; H. Zhang, W. H. Chan, A. W. M. Lee, W. Y. Wong, *Tetrahedron Lett.* **2003**, *44*, 395.
[50] E. Kleinpeter, F. Taddei, P. Wacker, *Chem Eur. J.* **2003**, *9*, 1360.
[51] J. Lin, W. H. Chan, A. W. M. Lee, W. Y. Wong, *Tetrahedron* **1999**, *55*, 13983.
[52] W. Oppolzer, *Tetrahedron* **1987**, *43*, 1969; *Erratum, ibid*. **1987**, *43*, 4057; O. Reiser, *Nachr. Chem. Tech. Lab*. **1996**, *44*, 612; O. Reiser, in 'Organic Synthesis Highlights IV', Ed. H. G. Schmalz, VCH, 2000, p. 11, 16.
[53] J. Raczko, M. Achmatowicz, P. Kwiatkowski, C. Chapuis, Z. Urbanczyk-Lipkowska, J. Jurczak, *Tetrahedron: Asymmetry* **2000**, *11*, 1027.
[54] L. M. Tolbert, M. B. Ali, *J. Am. Chem. Soc*. **1981**, *103*, 2104.
[55] J. Raczko, M. Achmatowicz, A. Jezewski, C. Chapuis, Z. Urbanczyk-Lipkowska, J. Jurczak, *Helv. Chim. Acta* **1998**, *81*, 1264.
[56] J. P. Foster, F. Weinhold, *J. Am. Chem. Soc.* **1980**, *102*, 7211; A. E. Reed, L. A. Curtis, F. Weinhold, *Chem. Rev.* **1988**, *88*, 899.
[57] A. D. Becke, *J. Chem. Phys.* **1993**, *98*, 5648; C. Lee, W. Yang, R. G. Parr, *Phys. Rev. B* **1988**, *37*, 785.
[58] M. D. Halls, H. B. Schlegel, *J. Chem. Phys.* **1999**, *111*, 8819.
[59] Gaussian 98, Revision A.7, M. J. Frisch, G. W. Trucks, H. B. Schlegel, G. E. Scuseria, M. A. Robb, J. R. Cheeseman, V. G. Zakrzewski, J. A. Montgomery Jr., R. E. Stratmann, J. C. Burant, S. Dapprich, J. M. Millam, A. D. Daniels, K. N. Kudin, M. C. Strain, O. Farkas, J. Tomasi, V. Barone, M. Cossi, R. Cammi, B. Mennucci, C. Pomelli, C. Adamo, S. Clifford, J. Ochterski, G. A. Petersson, P. Y. Ayala, Q. Cui, K. Morokuma, D. K. Malick, A. D. Rabuck, K. Raghavachari, J. B. Foresman, J. Cioslowski, J. V. Ortiz, A. G. Baboul, B. B. Stefanov, G. Liu, A. Liashenko, P. Piskorz, I. Komaromi, R. Gomperts, R. L. Martin, D. J. Fox, T. Keith, M. A. Al-Laham, C. Y. Peng, A. Nanayakkara, C. Gonzalez, M. Challacombe, P. M. W. Gill, B. Johnson, W. Chen, M. W. Wong, J. L. Andres, C. Gonzalez, M. Head-Gordon, E. S. Replogle, and J. A. Pople, Gaussian, Inc., Pittsburgh PA, 1998.
[60] P. L. Polavarapu, *J. Phys. Chem.* **1990**, *94*, 8106.

Received April 13, 2004